Chapter 38

Antennas for Medical Applications

Cynthia M. Furse

University of Utah

CONTENTS

38.1 OVERVIEW OF ANTENNAS FOR MEDICAL APPLICATIONS

Antennas used for medical applications span applications in imaging, communication with implantable medical devices, heating for treatment of cancer, cardiac abnormalities, and hypothermia, measurement of fields for assessment of RF safety, augmentation of healing, and reduction of pain. Some of these applications have gained worldwide acceptance and are currently used with human subjects, and others are still in the research and development stage. This chapter describes the nature of the human body environment in which these antennas are commonly used, relevant regulations and guidelines, and the antennas and their applications.

38.2 THE ENVIRONMENT

The Regulatory Environment

There are two types of regulations of particular interest to designers of antennas for medical applications. The first is the allowable frequency. Applications that are used external to the body or for short periods of time (hyperthermia treatment, pain control, cardiac ablation, etc.) utilize the Industrial, Scientific, and Medical (ISM) bands (433, 915, 2450 MHz) in both the United States and Europe. Higher frequencies have the advantage of smaller antenna sizes, but the disadvantage of lower depths of penetration within the body. Implantable medical devices that are meant to stay in the body for a long period of time have been allocated a band of their own in the United States, the Medical Implant Communication Service (MICS) band from 402–405 MHz.[1] The maximum bandwidth that can be used by a single device is 300 kHz in this band. The maximum power limit is 25 μW Equivalent Radiated Power (ERP).[2,3] MICS shares its frequency allocation with the Meteorological Aids Service (METAIDS), which is used primarily by weather balloons, and is therefore specified for indoor use.

The second type of regulation of interest in the design of antennas for medical applications is the limit on allowable absorbed power in the body. The limits for whole-body exposure are generally not the limiting factor. Instead, limits on localized power are more critical. Localized power is defined by specific absorption rate (SAR), which is calculated as

$$\text{SAR}\ (W/\text{kg}) = \frac{\sigma|\bar{E}_p|^2}{2\,\delta} \tag{38-1}$$

where σ is the electrical conductivity of the tissue (S/m), $\bar{E}_p$ is the peak value of the electric field, and δ is the density of the tissue (kg/m^3). Localized SAR for nontherapeutic applications is limited to 2 W/kg in any 10-gram region of the body with an approximately cubic volume.[4,5,6] An important exception is made in the new IEEE Safety Standard[5] for the pinna (the outer ear) for an increased limit of 4.0 W/kg for the general public and 20.0 W/kg for occupational exposures. For therapeutic applications such as cardiac ablation and hyperthermia, the absorption limit does not apply, and care must then be taken not to damage surrounding tissues by overheating them.

The question of whether electromagnetic radiation causes harm to the body at nonthermal levels has been hotly contested and remains a topic of ongoing research. A focused

review of this research was completed by the NIEHS in 1999.[7] Significant research and ongoing professional oversight have lead to today's RF exposure standards, which are meant to ensure safe levels of RF fields.[8] Still, designers of antennas for medical systems should be aware of public fears that may accompany their use and should anticipate being asked to address this question.

The Physical Environment

Antennas used for medical applications are strongly impacted by the lossy dielectric materials that make up the human body. This presents challenges when antennas are used for a communication system, because the tissues absorb the power and detune the antenna. This depends strongly on the frequency and the location and depth of the antenna in or near the body, and significant variation can be seen from patient to patient. Figure 38-1 shows the electrical properties of muscle and fat as a function of frequency.[9] At low frequencies, the conductivity of the tissue dominates the impact on the field, and at high frequencies, the dielectric values tend to dominate. Table 38-1[9] shows the electrical properties of several different tissues in the body at 433 MHz, which is a commonly used ISM frequency. Muscle is highly conductive and therefore very lossy, whereas fat has lower conductivity and therefore lower loss. These two tissues are near extremes in the body. A common rough approximation is that the body can be modeled using average properties of 2/3 muscle. This is suitable for addressing global questions such as total power absorbed in the body, but is generally not suitable for evaluating near field effects such as peak SAR.

The lossy tissues in the body have several effects on antennas used for medical applications. When antennas are used for deliberately depositing power in the body for hyperthermia or cardiac ablation, for instance, the power tends to stay more localized around the antenna, where it is absorbed and converted to heat. For cardiac ablation or in vitro hyperthermia applicators, this is good, because it means that the heat will not penetrate to nearby structures that are not meant to be heated. For external, whole-body applicators for hyperthermia or for medical imaging applications, this loss means that it can be difficult to get the power to penetrate deep within the body. Lower frequencies are used when possible, and regions near the surface of the body (such as the breast) are easier to work with than areas deep within the torso. Multiple antennas must be used outside the body and focused in some way in order to get the power deep into the body.

For biotelemetry (communication) applications, the same types of problems are seen. Communication with subcutaneous implants loses less power in the body than communication with deep body implants, for instance. Power lost in the body has two effects: it is wasted and cannot be used for communication, and the RF exposure limits typically limit

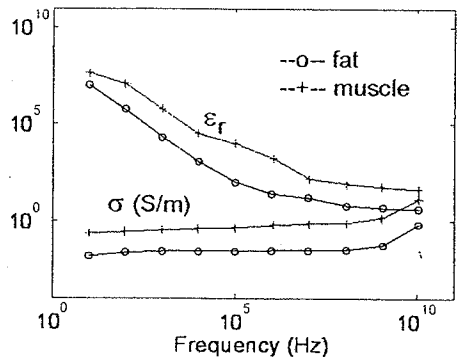

FIGURE 38-1 Electrical properties of muscle and fat (from Gabriel[9])

TABLE 38-1 Electrical Properties of Tissues at 433 MHz (from Gabriel[9])

Tissue	ε_r	σ (S/m)
Aorta	49.15	0.7395
Bladder	17.67	0.3128
Blood	57.3	1.72
Bone (Cancellous)	21.08	0.02275
Bone (Cortical)	13.77	0.1032
Bone (Marrow)	5.137	0.03575
Breast Fat	5.62	0.04953
Cartilage	43.64	0.65
Cerebellum	52.9	0.91
Cerebro Spinal Fluid	68.97	2.32
Cervix	44.17	1.020
Colon	60.88	0.96
Cornea	54.4	1.070
Dura	51.03	0.8
Eye Tissues	57.69	1.010
Fat	5.028	0.04502
Gall Bladder	60.06	1.035
Gall Bladder Bile	76.55	1.613
Grey Matter	54.27	0.8775
Heart	60.74	0.9866
Kidney	57.3	1.152
Lens Cortex	52.75	0.6742
Lens Nucleus	38.76	0.38
Liver	50.34	0.68
Lung Deflated	52.83	0.7147
Lung Inflated	21.58	0.3561
Muscle	64.21	0.9695
Nerve	35.7	0.500
Ovary	51.55	1.033
Skin (dry)	42.48	0.5495
Skin (wet)	51.31	0.72
Small Intestine	74.1	2.053
Spleen	60.62	1.041
Stomach	74.55	1.120
Tendon	50.53	0.7554

TABLE 38-1 *Continued*

Tissue	ε_r	σ (S/m)
Testes	65.2	1.137
Thyroid	60.02	0.8183
Tongue	58.79	0.8993
Tracea	42.93	0.673
Uterus	64.73	1.117
Vitreous Humour	66.16	0.3931
White Matter	39.84	0.5339

the power that can be used for communication and hence the range or bandwidth of the system. Also, the lower the frequency used (to enable penetration and minimize power loss), the larger the antenna must be. Determining the exact impact of the body on the antenna generally requires precise calculation of the antenna in the presence of the human body. This typically requires numerical methods that are described in the next section.

Numerical Simulation of Antennas in or near the Human Body

Several methods for analyzing antenna arrays for medical applications exist.[10] For simple cases where the biological structure can be approximated as uniform or by very simple models such as layers or cylinders, classical methods such as analytical analysis[11,12] or method of moments[13,14] can be used. If the structure of the body varies so much that anatomically precise modeling is rendered imprecise by variation between individuals, these simple analyses can be used to determine an optimal array design for the range of expected variation between individuals. An example of this was done in Hadley[15] for design of coils for vascular MRI. Another example in which the body can be modeled as near-uniform is in the case of arrays for hyperthermia of the brain. In Furse and Iskander[16] stepped-impedance dipoles were modeled using method of moments in an homogenous brain with a localized (nonhomogenous) tumor. Method of moments with a simple pulsed basis function (which is the most numerically efficient form) has limitations for heterogeneous models, however, due to artificial charge buildup on the dielectric interfaces.[13] Higher-order basis functions can overcome this limitation, although the computational complexity is significantly increased.[17] In addition, the method of moments is very computationally expensive when heterogeneous models are evaluated. It requires $N \log N$ computations, where N is the number of cells in the model, including those making up the heterogeneous object.

A more efficient method for calculation of heterogeneous objects is the finite difference time domain (FDTD) method, which has led to its tremendous popularity for numerical bioelectromagnetic calculations. For example, a interstitial array of hyperthermia applicators simulated using method of moments[16] was simulated with a fraction of the computational resources using FDTD.[18] Several individual hyperthermia applicators have been simulated using FDTD.[19] FDTD requires N^2 computations, where N is a cell in the (normally cubical) FDTD grid. Unlike method of moments, every cell in space (including at least a minimal amount of air surrounding the model) must be included in the discrete model, so the total number of cells, N, is likely to be larger. However, the significant improvement in computational efficiency generally makes this trade-off favor FDTD for bioelectromagnetic simulations. Complete detailed analysis of breast cancer imaging modalities was also done

with FDTD,[20–43] as well as hyperthermia systems,[44] and evaluation of cell phones (including those with dual antennas) near the human head.[45,46] Antennas for implantation in the body (mostly microstrip or Planar Inverted F (PIFA) types) have been simulated with FDTD and in some cases optimized with genetic algorithms.[47] Deep hyperthermia applicators (annular phased arrays) have been simulated extensively with FDTD.[48,49]

Several FDTD developments have been important for bioelectromagnetic simulations, including the development of frequency-dependent methods $(FD)^2TD$,[50] low-frequency FDTD methods,[51] efficient FDTD computation,[52] and evaluation of temperature using the bioheat equation.[49]

Model development is one of the significant challenges of numerical bioelectromagnetics. Models have progressed from the prolate spheroidal models of the human used during the 1970s[53] to roughly 1-cm models based on anatomical cross sections used during the 1980s[54] to a new class of millimeter-resolution MRI-based models of the body that have been the hallmarks of research since the 1990s.[55–58] Today, probably the most widely used models are derived from the Visible Man Project.[59]

Once a tissue-segmented model has been chosen, the electrical properties of the tissues are defined. The properties of human tissue vary significantly with frequency, so it is essential to use data accurately measured at the frequency of interest. There is a wide range of published data on measured tissue properties,[53,60–71] and work is still underway to measure and verify these properties. These and other references are electronically searchable at the University of Utah Dielectric Database OnLine.[72]

38.3 ANTENNAS FOR MEDICAL IMAGING

One of the most promising uses of antennas in medical applications is for imaging the location of leukemia,[73] breast tumors,[20–43] and cardiac anomalies.[74,75] Microwave imaging methods rely on the fact that the electrical properties of normal and malignant tissue are significantly different[60–67] and that there is significant variation from tissue to tissue. Location of breast cancer shows particular promise, because its relatively low loss allows electromagnetic fields to propagate to the tumor and back, and the proximity of the tumor to the outer surface of the body means that the signal does not have more than a few inches to propagate. Two major microwave imaging methods utilize antenna arrays. Tomography[20–27] attempts to map a complete electrical profile of the breast, and confocal imaging[28–43] maps only the location of significant scatterers. Both of these methods have used antenna arrays made up of wideband elements to send and receive the test signals. Microwave thermography picks up the passive electromagnetic fields from the body.[76–92] Magnetic Resonance Imaging (MRI) uses a strong magnetic field to cause the magnetic dipoles in the body to precess and then uses an array of loops to pick up the fields when they relax back to their normal state.[11,93–113]

Tomography for Breast Cancer Detection

Microwave tomography is used to provide a complete spatial mapping of the electrical properties in the region of interest. During the acquisition phase, an array of antennas surrounds the region of interest. One of the antennas in the array is used to transmit a signal, normally a sine wave,[20] set of sine waves,[21–22] or a broadband signal,[23] and all of the other antennas are used to receive the reflected signal. The array is scanned so that each antenna transmits each frequency, and these signals are received by each of the other antennas. After all of the data has been acquired, it is processed by comparing the received data with what

would be expected from a simulated model of the region. A numerical "forward model" is used to predict how much power is transmitted from the transmit antenna, passes into and reflects from the breast/tumor model, and is received by the receive antenna. Originally, the simulated model is just a good guess for what might be present, generally a generic breast model with no tumor. The differences between the measured and expected received data are used to modify the original guess to obtain an ideal model that best matches the measured data. This "inversion" is used to predict what model could have produced the measured data.

Microwave tomography for breast cancer has been demonstrated by several groups.[20–27] In the Dartmouth system,[20] for instance, sine waves from 300–1000 MHz (being expanded to 3 GHz) are transmitted from a circular array of 16 transmit/receive monopole antennas, shown in Figure 38-2, to produce 2D reconstructed images of the breast. Quarter-wave monopole antennas (in the fluid) that were built by extending the inner conductor of semi-rigid coax were used for this application. Monopoles were chosen because they are easy to model as a line source in a 2D reconstruction algorithm with high accuracy.[20] Water-filled waveguide apertures have also been used for tomography, but the monopole antennas were found to be as accurate and easier to build.[24]

Microwave tomography has been validated experimentally.[27] The presence of 1.1- or 2.5-cm saline tubes (representing tumors) in excised breast tissue are seen to be clearly visible.[26] Objects as small as 4 mm in diameter have been imaged at 900 MHz.[27]

Confocal Imaging for Breast Cancer Detection

Confocal imaging for breast cancer detection is another exciting application of antenna arrays in medical imaging. Confocal imaging is similar to ground-penetrating radar. Unlike microwave tomographic imaging, this method does not provide a complete electrical mapping of the region of interest. Instead it identifies locations of significant scattering. This method typically uses a single antenna scanned in a flat array pattern above the breast or a cylindrical array of very small broadband antennas.[28] For planar imaging, the patient lies face up, and the antenna is physically scanned in a plane above the breast.[29–31] For cylindrical imaging, the patient lies face down, with the breast extending into the cylindrical array

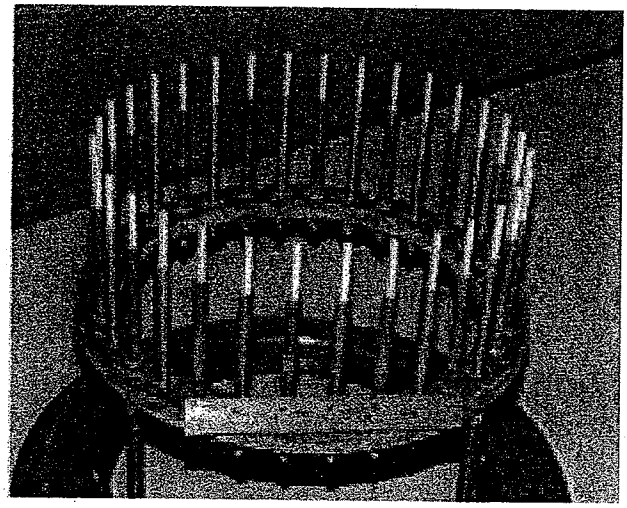

FIGURE 38-2 2D monopole array used for tomographic imaging of the breast (after P. M. Meaney et al[20] © IEEE 2000)

through a hole in the table.[32,33] Matching fluid surrounding the breast, similar to that used for microwave tomography, is suggested in this case. Both methods provide similar results.[33] One antenna in the array transmits an ultrawideband (UWB) pulse, which propagates into the breast, where it is reflected off significant electrical discontinuities, and is received in parallel by the other antennas in the array. Knowing the physical spacing between the array elements, the different delays between the transmit antenna, scattering point, and receiving antenna can be calculated geometrically. The received pulses representing a specific point in space can then be time delayed appropriately for each antenna, added up, and integrated to indicate the magnitude of the scattered energy from that point in space. This is effectively correlating the signals received from that point at all antennas.

The antennas used for confocal imaging must be UWB and small enough to fit within the relatively small array area. Resolution of less than 1 cm requires a bandwidth of at least 5 GHz. The lossy nature of tissue attenuates high-frequency signals, limiting the upper frequency to about 10 GHz. Initially, resistively loaded bowties were suggested for the planar configuration,[29–31,35,37] while dipole antennas were suggested for the cylindrical system.[32,33] Resistively loaded Vee dipoles have also been proposed.[36] In the cylindrical configuration, multiple antennas are present in the array, although they are not simultaneously active. In the planar system, a single antenna is scanned over the surface, creating a synthetic antenna aperture. To overcome the inherent inefficiency of resistively loaded antennas, a modified ridged horn antenna operating from 1 to 11 GHz has been introduced.[38] Most of the antennas are designed to observe copolarized reflections from the breast; however, two resistively loaded bowtie antennas in the shape of a Maltese cross, as shown in Figure 38-3, have also been proposed to pick up the cross-polarized reflections.[30] Cross-polarized reflections from simple tumor models were also examined.[34,39]

The antenna shown in Figure 38-3[34] consists of two cross-polarized bowtie antenna elements, an octagonal cavity behind the bowtie elements, and a metal flange attached to the cavity. The broadband bowties have flare angles of 45°. They are 1.67 cm long, which is a half-wavelength at 3 GHz in fat (similar to breast). The octagonal cavity blocks waves radiated away from the breast. The cavity is approximated as a circular waveguide filled with fat material for matching and size reduction. The first cutoff frequency is set to be

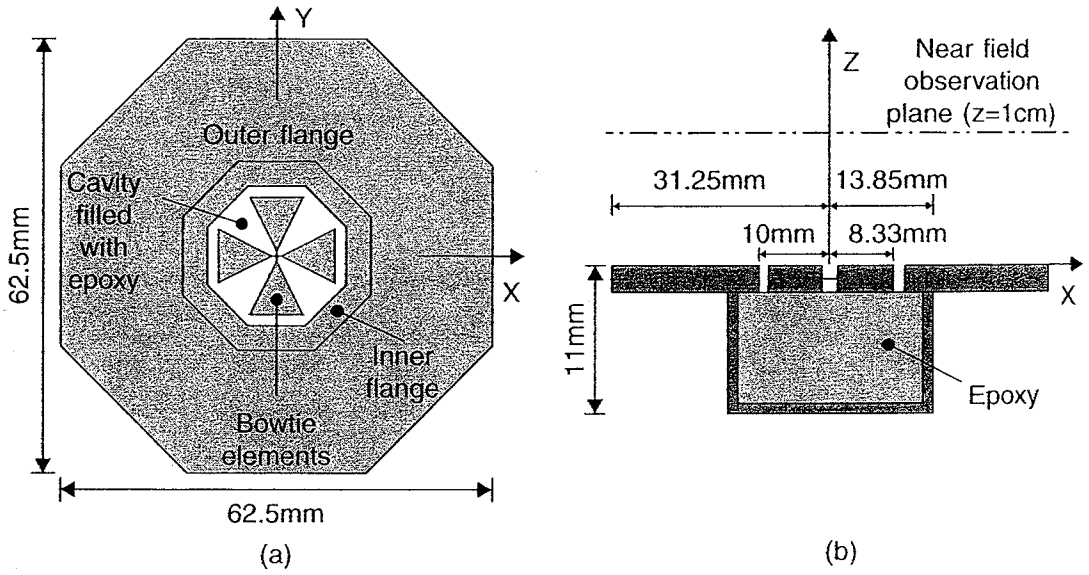

FIGURE 38-3 Cross-polarized antenna for confocal imaging. The properties of the substance inside the cavity and the medium outside the antenna are similar to fat ($\varepsilon_r = 9$; $\sigma = 0{:}2$ S/m) (after X. Yun et al[34] © IEEE 2005).

2 GHz for 2 to 4 GHz operation. The cavity length is a quarter wavelength, which is 11 mm at 3 GHz. The flange consists of an inner and outer component, and is designed to block unwanted waves such as surface waves. The antenna performance does not change significantly when the flange size is varied between 10–6.25 mm, therefore, the width of the outer flange is set to be 6.25 mm. The inner flange is designed to prevent possible electric field overshoot at the inner corners of the opening of the octagonal cavity or at the ends of the bowtie elements. A slotline bowtie antenna has also been proposed.[40]

A resistively loaded monopole antenna, shown in Figure 38-4, suitable for use in a cylindrical array was proposed by Sill and Fear.[41–43] Based on the Wu–King design[114–115] this antenna was designed to be usable from 1 to 10 GHz immersed in canola oil ($\varepsilon_r = 3.0$) for matching to breast tissue. The antenna is fabricated using high-frequency chip resistors (Vishay 0603HF, by Vishay Intertechnology, Malvern, PA) soldered to a high-frequency substrate (Rogers RO3203 series by Rogers Corporation, Chandler, AZ). The substrate ($\varepsilon_r = 3.02$ and $\sigma = 0.001$ S/m) has electrical properties similar to those of the canola oil. The antenna is soldered to a subminiature A (SMA) connector and attached to a metal plug for connection into the oil-filled test canister.

The cylindrical confocal imaging system has been experimentally tested.[41,43,116] Simulated tumors as small as 4 mm have been detected using a 3D system.

Microwave Radiometry

Microwave radiometry is a passive method where the natural electromagnetic radiation or emission from the body is measured to allow detection or diagnosis of pathogenic conditions.[77] This method has been proposed for detection of breast cancer[80,90,91] and brain cancer,[81] in which the metabolism of cancer cells increases the localized temperature 1 to 3°C. This method has also been used for fluid and blood warming,[77] for detection of rheumatology,[79] and for monitoring temperature rise during hyperthermia treatment.[78]

Typical antennas include open-ended rectangular waveguides,[82–85] small-loop antennas,[87] and a horn antenna with a dielectric lens.[88] Working around 3 GHz, all of these antennas have radiation patterns that have minimal penetration into the body, thus strongly weighting them to monitoring of surface temperatures.[89,92] Increased focus, and therefore better spatial accuracy, was obtained with an array of six rectangular aperture antennas filled with low-loss

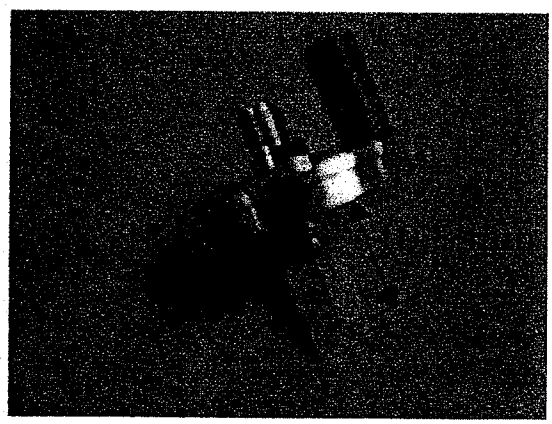

FIGURE 38-4 Fabricated resistively loaded monopole antenna soldered to an SMA connector and attached to a metal plug (after J. M. Sill and E. C. Fear[43] © IEEE 2005)

dielectric ($\varepsilon_r = 25$), which were scanned over the object of interest in an overlapping pattern. Preliminary results indicated promise for location of breast tumors.[90–91]

Magnetic Resonance Imaging

Magnetic Resonance Imaging (MRI) uses a very strong magnetic field (0.5T, 1.5T, 3T, 4T, 7T, perhaps in the future 8T) to make the magnetic dipoles in the body precess (line up). When they are released, a set of receiver coils picks up the magnetic field created when these dipoles return to their normal orientations (position may change a lot as in blood imaging, diffusion, etc.). The relaxation properties of the different tissues affect the relative received signal intensities, and a 3D map of the body can be produced.

There are two basic types of receiver coils used for MRI. Volume coils, such as the quadrature birdcage head coil shown in Figure 38-5,[11] are used for imaging large and deep anatomic structures of the body and provide homogeneous field profiles. For high-resolution applications that are more localized, such as angiographic imaging, hypocampus imaging, and functional imaging, in which the object features are very small, volume coils pick up less signal and more noise, thus having a lower signal-to-noise ratio (SNR) and poor-quality images. Modifications such as the use of an RF reflector or "endcap,"[11] and modified shapes such as the elliptical[94] or "dome"[95,96] coils, have been developed. Smaller-volume surface coils[97] have been shown to improve image quality, particularly when combined into phased arrays[98–106] such as the one shown in Figure 38-6. Phased-array coils are closer to the area of interest, so they pick up larger signal strength, and are smaller, so they pick up less noise, thus having a higher SNR. They are designed to overlap so that the mutual inductance between coils is zero, and so that the impedance at the preamplifier is very low, for optimal SNR.[8] Part of the price for this improved image quality is the complexity of the receiver and data acquisition system, as each antenna is received on an individual channel. The image processing is also more computationally expensive, as the signal from each antenna is weighted depending on its proximity to the target region (and hence expected relative SNR), phase shifted, and combined with the other similarly processed signals.

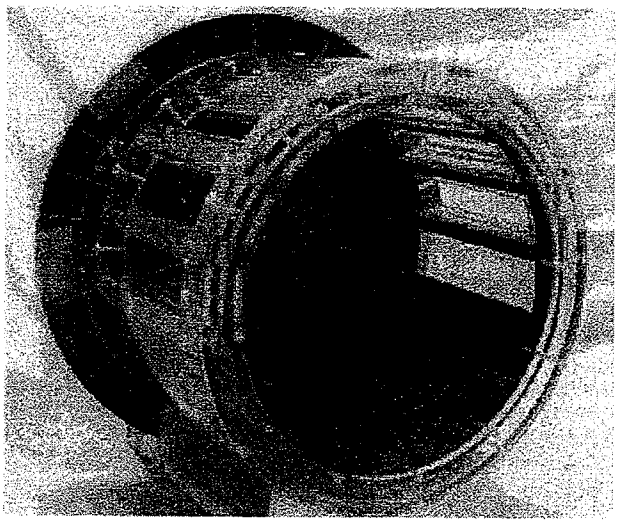

FIGURE 38-5 Quadrature birdcage coil with endcap used for whole-volume head imaging (reprinted with permission from J. R. Hadley et al[11] © *Journal of Magnetic Resonance Imaging* 2000)

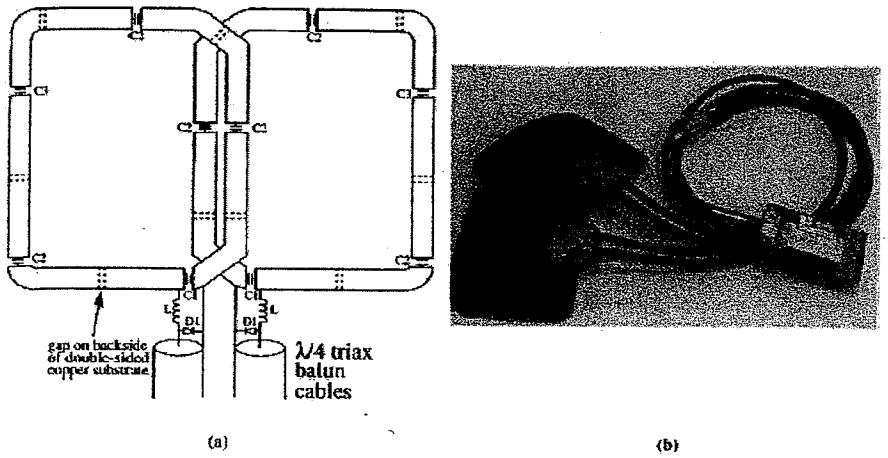

FIGURE 38-6 (*a*) Two-element phased-array coil design. Dashed lines indicate the breaks in the underside of the double-sided copper section of the coil. (*b*) Image of finished phased-array coils (enclosed in foam) with triax balun cables and phased-array port connector box (reprinted with permission from J. R. Hadley et al[11] © *Journal of Magnetic Resonance Imaging* 2000).

Among the practical considerations that are challenging with phased-array coils are the data acquisition time and the limited field of view, particularly for applications where the region of interest (an arterial occlusion, for instance) may not be precisely known and is therefore easy to miss. Phased-array coils have been used for numerous magnetic resonance angiography (MRA) applications including peripheral[107,108] abdominal, intracranial, and carotid imaging.[109–111] Recent coil designs have started to integrate phased-array elements into volume-like coils with the ability to control how the image is constructed to achieve maximum image quality.[112,113] For these applications, the coil array functions much like the phased array in a synthetic aperture radar application. The image quality for the different coil types and configurations depends strongly on the application. The optimal image construction algorithm depends strongly on the application and region of interest, making the flexibility of being able to synthetically develop large or small subarrays very attractive.

38.4 HEATING

Hyperthermia

Hyperthermia (HT)[117,118] is a method of treating cancer by heating the body. The tissue is typically heated to 41 to 45°C for 30 to 60 minutes. Often, this involves focusing the energy on the tumor region, relying on the tumor to be more sensitive to heat than the surrounding healthy tissues. This may be due to poor internal vasculature of the tumor or its higher conductivity and permittivity caused by increased water and ionic content. HT has also been shown to increase the effectiveness of radiation or chemotheraphy.[119–120] The most commonly used frequencies for hyperthermia are 433, 915, and 2450 MHz. The type of antenna or antenna array used for HT depends on whether it is to be administered superficially, interstitially, or deep-body.

Superficial HT applicators include microstrip,[121] waveguide,[122] current sheets,[123] inductive,[124] and the dual concentric conductor antenna, or DCC, shown in Figure 38-7.[125–128] The DCC is particularly attractive, because it can be easily fabricated on flexible, printed,

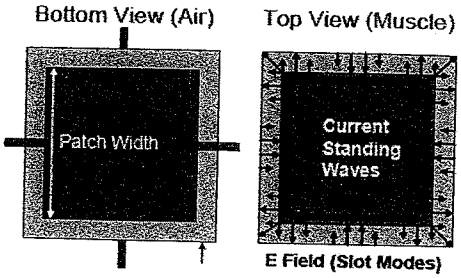

FIGURE 38-7 DCC antenna geometry, E fields in the ring slot and edge currents (after P. F. Maccarini et al[126] © IEEE 2004)

circuit-board material, which makes it easy to conform to virtually any part of the human body. The DCC aperture is a ring-slot configuration fed simultaneously on all four sides. Prediction and optimization of the heating is normally done by analyzing the near fields of the antenna (the heating region) numerically.[126]

Interstitial applicators for HT are typically monopole antennas made from coaxial cables with the center conductor extending beyond the outer ground shield of the cable.[129] These antennas have a tear-drop-shaped radiation pattern, so the majority of the heating is near the feedpoint of the antenna (where the ground shield stops), leaving the tip of the antenna extended beyond the useable heating range. The heating distribution can be made more uniform by varying the width of the conductor[16] or adding a choke to the antenna.[130] Numerous other designs of interstitial applicators also exist. The heating pattern can be adjusted within the array by phasing the antenna elements[16] or by using nonuniform insulation.[131]

Deep-body HT applicators are generally based on annular phased arrays (APA) of waveguides,[118] coaxial TEM apertures,[132] printed antennas,[129,133] and induction systems.[134] Originally, APA systems contained only one ring of 2D applicators surrounding the patient. The ring could be scanned vertically. Significant improvement with a true 3D HT system with the applicators vertically offset has been observed.[129] The first clinically used 3D-type applicator is the SIGMA-Eye applicator (BSD Medical Corp., Salt Lake City, UT[135]). A detailed description of this applicator and different numerical antenna feed models can be found in Nadobny et al.[136]

Among the ongoing antenna design challenges in this area is the design of antennas that can be used to also monitor temperature and administer radiation therapy.[128,133,137] One prototype combination device is shown in Figure 38-8 and another in Figure 38-9. Another research area is the use of optimization approaches to predict and control the heating pattern.[138,139]

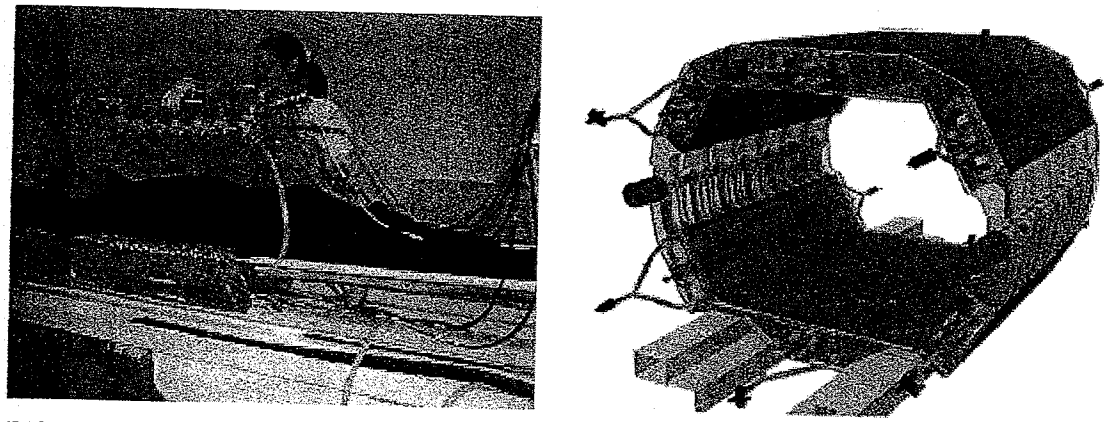

FIGURE 38-8 A prototype of the new Berlin MR-compatible Water-Coated Antenna Applicator (WACOA) (after J. Nadobny et al[137] © IEEE 2005)

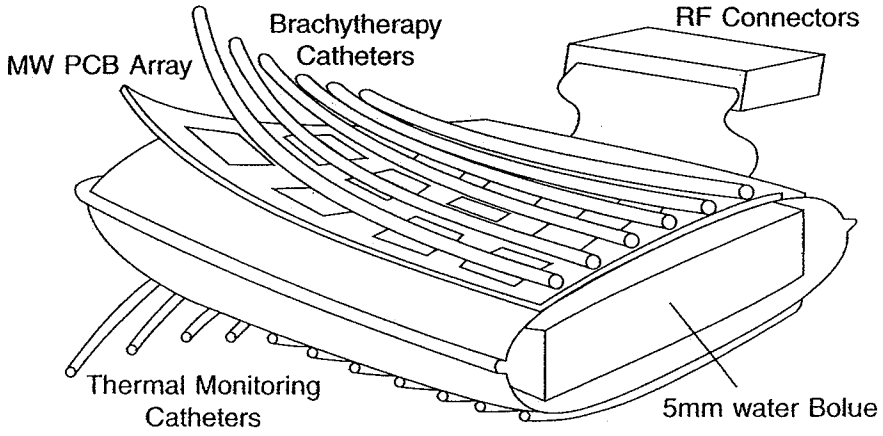

FIGURE 38-9 Schematic of combination applicator showing component parts: parallel catheter arrays for brachytherapy sources and thermal mapping sensors, PCB antenna array, and water coupling bolus (after P. Stauffer et al[133] © IEEE 2004)

Treatment of Hypothermia

Patients who have experienced hypothermia are at great risk during the rewarming process. Conventional methods such as warm water baths use external sources of heat, which warm the peripheral regions while the heart is still cold. The demand for increased circulation to the extremities can overload the heart. EM applicators can produce deeper heating than methods that simply heat the body surface and rely on thermal conduction to carry the heat to the deeper tissues. EM heating provides heat deeper into the body, which increases cardiac output and circulates warmed blood to the peripheral tissues without overloading the heart.[140]

Cardiac Ablation

Microwave catheter ablation uses monopole antennas inserted in catheters to the heart to treat cardia arrhythmias by creating deep lesions that destroy the source of the arrhythmias. Frequencies of 915 or 2450 MHz are typically used.[141,142] Ablation requires localized temperatures of 50–90° C for a short time, typically a few minutes. Microwave ablation has also been used in conjunction with traditional balloon angioplasty to soften arterial plaque.[143]

38.5 COMMUNICATION (BIOTELEMETRY)

Wireless communication systems and their associated implantable antennas are needed for communication with implantable medical devices such as cardiac pacemakers and defibrillators,[144] neural recording and stimulation devices,[145] and cochlear[146] and retinal[147] implants. Designing antennas for embedded applications is extremely challenging because of reduced antenna efficiency, impact of the environment on the antenna, the need to reduce antenna size, and the very strong effect of multipath losses. In addition to the present needs for embedded antennas, the expansion of MEMS, which are expected to play a dominant role in next-generation technologies, will add dramatically to the applications for imbedded antennas. Ultra-small devices (small enough to be injected in a human vein, for instance) and the desire to communicate with them will inevitably lead to the need for miniaturized antennas embedded in lossy environments. Emerging medical telemetry devices have led

to recent advances in the design of small, biocompatible antennas that can be implanted in the human body.[148–175]

Major challenges exist for implantable antennas. Not only do they have to be long-term biocompatible, but they must also be small, passive or highly efficient (to reduce battery requirements inside the body), and able to transmit power through the highly lossy body structure. In addition, they must meet the maximum SAR guidelines, which can be quite challenging. The very near field of the antenna is the inductive zone where power is not radiated. If lossy material is in the inductive zone of the antenna, which it normally is for implanted antennas, this near field power is absorbed and shows up in the SAR measurements or calculations. Thus, SAR is often the limiting factor for power transmitted from an implanted device.

In the majority of wireless telemetry cases for implantable devices, inductively coupled coils often wound around a dielectric or ferrite core are used.[152–167,176] In these cases, the time-varying magnetic field generated by the primary coil is received by the secondary coil, which results in an induced current in the implanted coil. Frequencies are often lower than 50 MHz to ensure that the presence of the human body does not significantly obstruct the coupling between the coils. In this case, the most important parameters for the design of the telemetry system are the self and mutual inductances of the coils. Several methods can be used to determine these parameters depending upon the frequency of interest and the geometrical shape of the coils. For the simplest traditional coil geometries (circle, square), analytical approximations of self and mutual inductances are often used, whereas more sophisticated methods (such as the partial inductance method and similar methods) can be used in the case of geometrically complex coils. A measure of the quality of coupling between two coils is given by the coupling coefficient K between two coils ($0 \le K \le 1$), defined by

$$K = \frac{M_{12}}{\sqrt{L_1 L_2}}$$

where M_{12} is the mutual coupling between coils 1 and 2, and L_i is the self inductance of coil i. To maximize the power delivered to the load in these applications, usually a capacitor is inserted in parallel with the inductance of the coil and the resistance of the load to form a parallel resonant LC circuit. Many other parameters may affect the design of inductively coupled coils for biomedical telemetry systems, such as implant size, maximum power, temperature increase in the implanted device, and specific absorption rate of power (SAR given in W/kg) induced in the tissue.[177]

Most inductive telemetry links are used for subcutaneous applications due to power restrictions for passive devices. Data rates are generally low, and size/weight and biocompatibility issues plague these devices. However, recent advances continue to reduce the power requirements and provide more biocompatible designs. The Utah Electrode Array (UEA), for example, uses a pickup coil printed on a ceramic substrate and integrated with the implanted neural electrode array, as shown in Figure 38-10.[145] The implanted coil is energized by an external inductive programmer/reader that powers the implanted circuitry while transferring telemetry data.

Radiofrequency links are also being developed for communication with medical implants. For cardiac telemetry, a dipole[171] and spiral or serpentine microstrip,[173,174] and a waffle-type patch[178] have been designed for implantation in the shoulder. An insulated wire antenna has also been used, and this wire may be used as the lead between the heart and the battery pack/controls of the pacemaker.[168] The antenna can be treated as a waveguide, where the lossy body acts as the outer conductor of the waveguide. The insulated antenna in tissue may be matched with a load resistor connected to the conducting tissue in order to reduce or eliminate the reflection.[169]

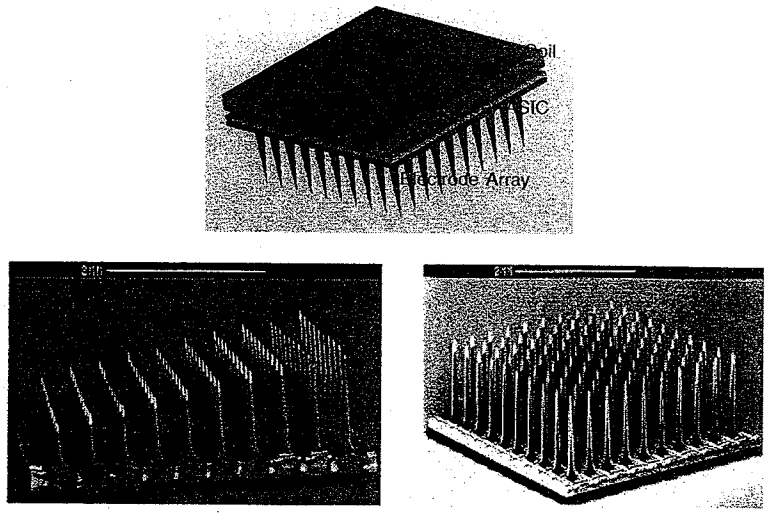

FIGURE 38-10 Utah Electrode Array packaged with a custom ASIC and printed receiver coil (after K. Guillory and R. A. Normann[145] ©*J. Neurosci. Methods* 1999)

Another type of antenna used for communication with cardiac devices is the circumference antenna, which is a monopole antenna that is mounted around the edge of the pacemaker case, as shown in Figure 38-11.[169,170] The 94-mm-long circumference antenna shown in Figure 38-11 was centered in a plastic insulator with a thickness of 10 mm. The bandwidth where the SWR of this antenna is less than 2 is 42 MHz, which is larger than the required MICS allocation of 3 MHz.

For smaller implants, a microstrip patch antenna has been successfully used for a retinal prosthesis,[175] and a small dipole has been designed for communication with a brain implant.[172]

Deep-torso devices will experience more loss than subcutaneous devices. Furthermore, the location in the body controls the radiation pattern shape as well as magnitude. For example, the calculated radiation patterns for a small, multiturn loop antenna implanted in

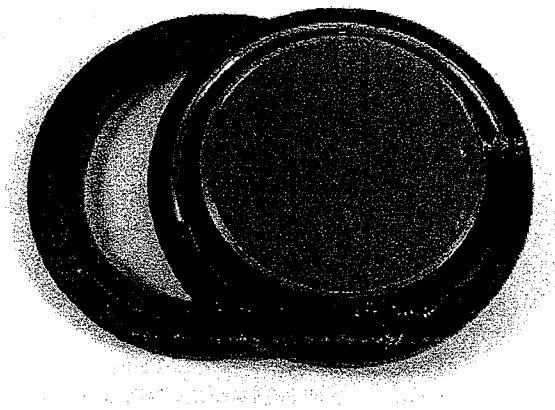

FIGURE 38-11 Circumference antenna on a pacemaker model (after A. Johansson,[169] Figure 5-3)

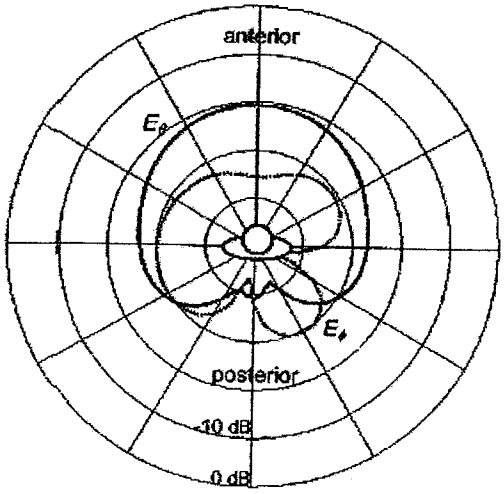

FIGURE 38-12 Calculated azimuthal radiation patterns for a 418-MHz vertical source: vertically polarized pattern (solid line) and horizontally polarized pattern (dotted line) (after W. G. Scanlon et al[156] © IEEE 2000)

the vagina are shown in Figure 38-12. Measured net body losses (power absorbed in the body) for this 418-MHz antenna are 19.2 dB. The bodyworn radiation efficiency is

$$\eta_b = \frac{P_{\text{body}}}{P_{\text{air}}} = 1.2\%$$

where P_{air} is the total power radiated by the antenna in air, and P_{body} is the total power radiated (external to the body) by the antenna implanted in the body. At 916.5 MHz, the measured net body loss is 24.3 dB, and the bodyworn radiation efficiency is 0.37 percent.[156] The substantial losses in the body have so far limited deep-torso implants to communication with receivers held on or very near the body.

38.6 PULSED ELECTROMAGNETIC FIELDS

Pulsed electromagnetic fields (PEMFs) have been developed for a number of medical applications. These fields are generally delivered by electrodes connected directly to the body, and as such are not truly an application of antennas. However, since this method is showing significant promise for many different medical applications, and since UWB antennas are being used in many other areas, it is not unlikely that antenna design concepts could be applied to PEMF applicators in future applications.

Bone and Tissue Healing

Pulsed electromagnetic fields have been found to be highly effective for healing fractures and soft-tissue injuries, particularly those that do not respond to ordinary healing methods. As early as 1812, passing "electric fluids" through needles inserted in the fracture gap was found to stimulate bone healing, and by the mid-1800s, this DC current stimulation was

considered the method of choice for slow-healing fractures. Today's bone-healing PEMF systems typically use a 72-Hz single-pulse pattern. While the full biological mechanism is not minutely understood, it appears PEMFs of this type are able to retard the osteoclasts that destroy bone while increasing the rate of new bone formation.[179]

Pain Control

Pulsed electromagnetic fields have also been used for controlling pain. Electrodes are placed strategically around the knee, shoulder, back, etc., and PEMF is applied. This has been found to provide both short- and long-term pain relief, although the exact reason is not fully understood. This method is currently used in both human and veterinary medicine.[179]

Drug Delivery and Electrochemotherapy

Pulsed electromagnetic fields can be used for a wide variety of needle-less drug delivery applications. Iontophoresis is a method to electrically force drugs across a transdermal interface using a relatively small voltage (0.1–10 V) across the skin boundary. This method appears not to create structural changes in the cells or the skin, but rather just creates ion pathways that a conductive fluid (drug) will follow through pre-existing aqueous pathways. At present, a limited number of drugs can be delivered using this method.[180]

Pulsed electromagnetic fields can also be used to treat cancer, using a new therapy called electrochemotherapy, which has been used for a variety of cutaneous tumors, including head and neck tumors, melanomas, superficial breast cancer lesions, etc. In this therapy, the resistance of malignant cells to penetration by certain chemotherapeutic agents is temporarily lowered by electroporation, which creates temporary pores (pathways) in the membranes of the malignant cells by the application of short DC pulses that generate electric fields of several kV/cm. Once the cells are porated, the chemotherapeutic agents can enter the malignant cells and destroy them. Electrochemotherapy not only can increase the efficacy of certain chemotherapeutic agents, but also can reduce side effects because malignant cells can be destroyed with much lower doses of chemotherapeutic agents than with conventional chemotherapy.[180,181]

38.7 SENSING

In addition to receiving and transmitting power for communication or imaging and depositing power for heating applications, antennas can be used as sensors. Antennas are used as probes for dielectric properties and electric or magnetic fields.

Dielectric Measurement Probes

Measurement of the electrical properties of tissues has been done extensively to facilitate research, numerical modeling, etc. High-frequency in vivo and in vitro dielectric measurements of tissue are typically made using an open-ended coaxial probe.[182] The coaxial probe is sensitive to material that lies within a fringing capacitance zone adjacent to the probe tip. A two-wire, dipole-type probe has also been used.[183] Another application of dielectric property measurements is in vivo measurement of brain fluid.[184]

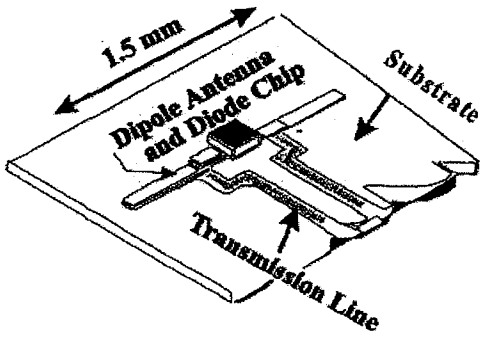

FIGURE 38-13 Miniature printed dipole antenna for measurement of electric fields to determine cell phone RF exposure compliance (H. Bassen and G. Smith[185] © IEEE 1983)

Electric and Magnetic Field Probes

Miniature electric field probe antennas have been designed for assessment of compliance of electromagnetic devices with RF exposure guidelines.[185] Measurement of SAR requires evaluation of the localized electric field, which should not be perturbed by the probe. This requires a very tiny electric or magnetic field receiver, such as the one shown in Figure 38-13. Because this probe is inherently sensitive to the polarization of the electric field, three perpendicular probes are used, as shown in the SPEAG probe in Figure 38-14. A magnetic field probe is also shown in this figure, with three perpendicular receiving loops.[186]

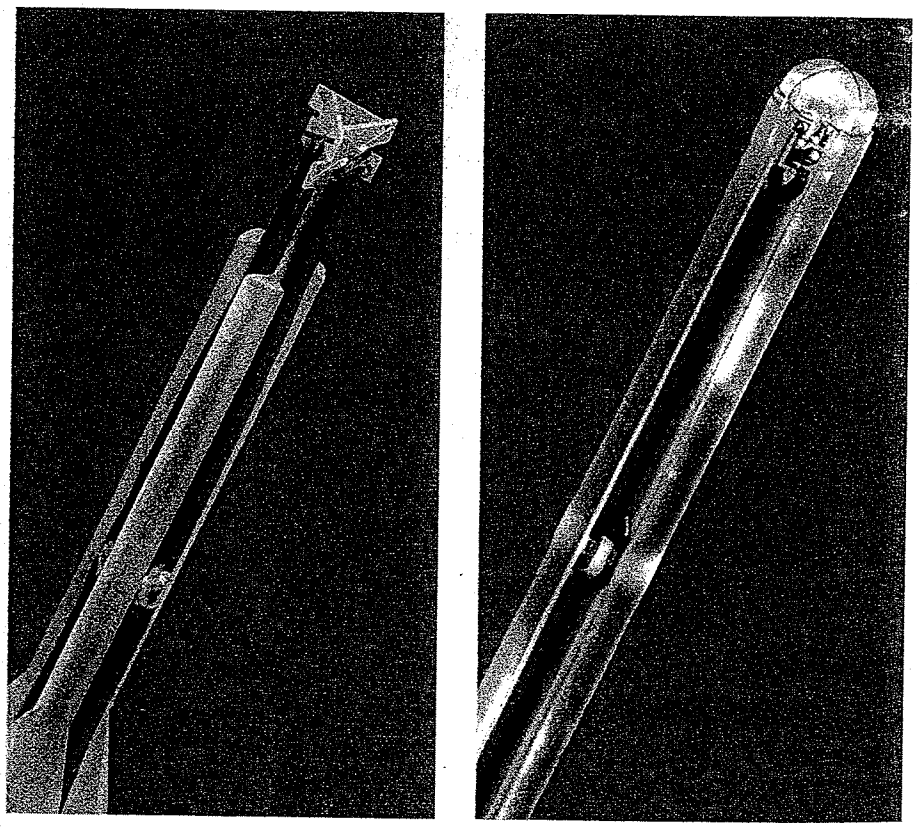

FIGURE 38-14 Electric and magnetic field probes from SPEAG (reprinted with permission, Schmid & Partner Engineering AG, Zurich)

38.8 FUTURE DIRECTIONS

The medical applications of antennas described in this chapter are by no means all inclusive. New technology is rapidly being developed, and creative new ideas continue to emerge. The basic capabilities of antennas to transmit information, deliver heat, sense electrical properties, and receive information for imaging will continue to lead to new applications for antennas in medicine. At the risk of tabloid-type predictions, the following are some expectations for where antennas will continue to grow in medical applications.

Communication with medical devices is an area that is rapidly expanding. The first medical devices were cardiac devices that had large battery packs and control systems and minimal data up/downlink requirements that could be managed in a doctor's office. Today these devices are pressing for higher data rates, real-time communication, and more efficient links. Their size has been continually shrinking and promises to shrink radically, due mainly to advances in battery technology. Emerging nerve stimulation or recording devices require far less power than cardiac devices, and therefore do not require batteries at all. Prosthetic nerve devices hold promise for artificial vision, hearing, smell, balance and muscle control, nerve "repair," and a new level of treatment of brain malfunction for Parkinson's disease, depression, epilepsy, and more. New packaging techniques and ultra-efficient electronics are driving the need for superminiaturized antennas. This demand is likely to grow dramatically with the success of microscale electronics, microfluidics, and microscale sensors and actuators. Smart pills have shown the capability of "untethered" communication systems in the body, and other applications are likely to utilize this freedom in the future, such as moving through the bloodstream for diagnosis or treatment.

Devices used for heating have either been large, external devices that attempt to focus power, or much smaller devices inserted through a vein/artery or laproscopic surgical opening. These devices are also likely to shrink in size with the miniaturization of electronics, providing opportunity for more precise control of heat delivery.

Although medical imaging is a relatively mature field, new methods and radical enhancements to mainstream methods continue to emerge. New antenna designs for imaging tend to be larger numbers (arrays) of small antennas. Enhancing the bandwidth while miniaturizing the antenna continues to be a focus in many applications. Arrays that are nonuniform and nonplanar are likely to be important in many applications. With the ability to place antennas in the body for medical implant devices, it would not be surprising to see the development of imaging systems that can be swallowed, injected, or placed in body orifices for better imaging of sensitive structures.

Antennas are an integral part of medical devices today, and hold promise to play a significant role in the development of emerging devices for future medical systems.

Acknowledgments

Several researchers have contributed to this chapter, including Dr. Gianluca Lazzi (inductive coil telemetry), Jeff Johnson and Dr. Pichitpong Soontornpipit (biomedical telemetry), and Dr. Rock Hadley (MRI).

REFERENCES

1. Medical Implant Communications Service (MICS) Federal Register, "Rules and Regulations," vol. 64, no. 240 (Dec. 1999): 69926–69934.
2. International Telecommunication Union, Recommendation ITU-R SA.1346, 1998.

3. "Planning for Medical Implant Communications Systems (MICS) and Related Devices," Proposals Paper SPP 6/03, Australian Communications Authority.
4. M. H. Repacholi, *Biological Effects and Medical Applications of Electromagnetic Energy*, Chap. 2, O. P. Gandhi (ed.) (Englewood Cliffs, NJ: Prentice-Hall, 1990).
5. *IEEE Standard for Safety Levels With Respect to Human Exposure to Radiofrequency Electromagnetic Fields, 3 kHz to 300 GHz*, IEEE Std. C95.1, 1999, revised to *Standard for Safety Levels with Respect to Human Exposure to Radiofrequency Electromagnetic Fields, 3 kHz to 300 GHz*, IEEE Standards Coordinating Committee 28.4, 2006.
6. ICNIRP, "Guidelines for Limiting Exposure to Time-Varying Electric, Magnetic, and Electromagnetic Fields (up to 300 GHz)," *Health Phys.*, vol. 74 (1998): 494–522.
7. National Institute of Environmental Health Science, http://www.niehs.nih.gov/emfrapid/home.htm.
8. O. P. Gandhi, *Biological Effects and Medical Applications of Electromagnetic Energy*, Chap. 3, O. P. Gandhi (ed.) (Englewood Cliffs, NJ: Prentice-Hall, 1990).
9. C. Gabriel, "Compilation of the Dielectric Properties of Body Tissues at RF and Microwave Frequencies," Final Technical Report, Occupational and Environmental Health Directorate Radiofrequency Radiation Division, Brooks Air Force Base, TX, 1996.
10. O. P. Gandhi, *Biological Effects and Medical Applications of Electromagnetic Energy*, Chap. 6 (Englewood Cliffs, NJ: Prentice-Hall, 1990).
11. J. R. Hadley, B. E. Chapman, J. A. Roberts, D. C. Chapman, K. C. Goodrich, H. R. Buswell, A. L. Alexander, J. S. Tsuruda, and D. L. Parker, "A Three-Coil Comparison for MR Angiography," *Journal of Magnetic Resonance Imaging*, vol. 11 (2000): 458–468.
12. R. W. P. King, G. J. Fikioris, and R. B. Mack, *Cylindrical Antennas and Arrays* (Cambridge, UK: Cambridge Univ. Press, 2002).
13. H. Massoudi, C. H. Durney, and M. F. Iskander, "Limitations of the Cubical Block Model of Man in Calculating SAR Distribution," *IEEE Trans. Microwave Theory and Tech.*, vol. 32 (1984): 746–752.
14. C. T. Tsai, H. Massoudi, C. H. Durney, and M. F. Iskander, "A Procedure for Calculating Fields Inside Arbitrarily-Shaped, Inhomogeneous Dielectric Bodies Using Linear Basis Functions with the Moment Method," *IEEE Trans. Microwave Theory and Tech.*, vol. 34 (1986): 1131–1139.
15. J. Rock Hadley, "Design of Radio Frequency Coil Arrays for Optimal Signal to Noise Ratio for Magnetic Resonance Angiography," PhD dissertation, University of Utah Electrical and Computer Engineering Department, 2005.
16. C. M. Furse and M. F. Iskander, "Three-dimensional Electromagnetic Power Deposition in Tumors Using Interstitial Antenna Arrays," *IEEE Trans. on Biomedical Engineering*, vol. 36 (Oct. 1989): 977–986.
17. O. H. Schaubert, D. R. Wilton, and A. W. Glisson, "A Tetrahedral Modeling Method of Electromagnetic Scattering by Arbitrarily Shaped Inhomogeneous Objects," *IEEE. Trans. Antennas and Propagation*, vol. 32 (1984): 75–82.
18. P. Cherry and M. F. Iskander, "FDTD Analysis of Power Deposition Patterns of an Array of Interstitial Antennas for Use in Microwave Hyperthermia," *IEEE Trans. Microwave Theory and Tech.*, vol. 40, no. 8 (Aug. 1992): 1692–1700.
19. J. C. Camart, D. Despretz, M. Chive, and J. Pribetich, "Modeling of Various Kinds of Applicators Used for Microwave Hyperthermia Based on the FDTD Method," *IEEE Trans. Microwave Theory and Tech.*, vol. 44, no. 10 (Oct. 1996): 1811–1818.
20. P. M. Meaney, M. W. Fanning, D. Li, S. P. Poplack, and K. D Paulsen, "A Clinical Prototype for Active Microwave Imaging of the Breast," *IEEE Trans. Microwave Theory Tech.*, vol. 48 (Nov. 2000): 1841–1853.
21. W. C. Chew and J. H. Lin, "A Frequency-Hopping Approach for Microwave Imaging of Large Inhomogeneous Bodies," *IEEE Microwave Guided Wave Lett.*, vol. 5 (Dec. 1995): 439–441.
22. O. S. Haddadin and E. S. Ebbini, "Imaging Strongly Scattering Media Using a Multiple Frequency Distorted Born Iterative Method," *IEEE Trans. Ultrason., Ferroelect., Freq. Contr.*, vol. 45 (Nov. 1998): 1485–1496.

23. Q. Fang, P. M. Meaney, and K. D. Paulsen, "Microwave Image Reconstruction of Tissue Property Dispersion Characteristics Utilizing Multiple-Frequency Information," *IEEE Trans. Microwave Theory Tech.*, vol. 52 (Aug. 2004): 1866–1875.

24. P. M. Meaney, K. D. Paulsen, A. Hartov, and R. C. Crane, "An Active Microwave Imaging System for Reconstruction of 2-D Electrical Property Distributions," *IEEE Trans. Biomed. Imag.*, vol. 42 (Oct. 1995): 1017–1026.

25. K. D. Paulsen and P. M. Meaney, "Compensation for Nonactive Array Element Effects in a Microwave Imaging System: Part I—Forward Solution vs. Measured Data Comparison," *IEEE Trans. Med. Imag.*, vol. 18 (June 1999): 496–507.

26. P. M. Meaney, K. D. Paulsen, M. W. Fanning, and A. Hartov, "Nonactive Antenna Compensation for Fixed-Array Microwave Imaging: Part II—Imaging Results," *IEEE Trans. Med. Imag.*, vol. 18 (June 1999): 508–518.

27. P. M. Meaney, K. D. Paulsen, A. Hartov, and R. K. Crane, "Microwave Imaging for Tissue Assessment: Initial Evaluation in Multitarget Tissue-Equivalent Phantoms," *IEEE Trans. Biomed. Eng.*, vol. 43 (Sept. 1996): 878–890.

28. E. C. Fear, S. C. Hagness, P. M. Meaney, M. Okieniewski, and M. Stuchly, "Enhancing Breast Cancer Detection Using Near Field Imaging," *IEEE Microwave Magazine* (March 2002): 48–56.

29. S. C. Hagness, A. Taflove, and J. E. Bridges, "Two-dimensional FDTD Analysis of a Pulsed Microwave Confocal System for Breast Cancer Detection: Fixed-Focus and Antenna-Array Sensors," *IEEE Trans. Biomed. Eng.*, vol. 45 (Dec. 1998): 1470–1479.

30. S. C. Hagness, A. Taflove, and J. E. Bridges, "Three-dimensional FDTD Analysis of a Pulsed Microwave Confocal System for Breast Cancer Detection: Design of an Antenna-Array Element," *IEEE Trans. Antennas Propagat.*, vol. 47 (May 1999): 783–791.

31. X. Li and S. C. Hagness, "A Confocal Microwave Imaging Algorithm for Breast Cancer Detection," *IEEE Microwave Wireless Comp. Lett.*, vol. 11 (March 2001): 130–132.

32. E. Fear and M. Stuchly, "Microwave System for Breast Tumor Detection," *IEEE Microwave Guided Wave Lett.*, vol. 9 (Nov. 1999): 470–472.

33. E. C. Fear and M. A. Stuchly, "Microwave Detection of Breast Cancer," *IEEE Trans. Microwave Theory Tech.*, vol. 48 (Nov. 2000): 1854–1863.

34. X. Yun, E. C. Fear, and R. H. Johnston, "Compact Antenna for Radar-Based Breast Cancer Detection," *IEEE Trans. Antennas and Propagation*, vol. 53, no. 8 (Aug. 2005): 2374–2380.

35. S. C. Hagness, A. Taflove, and J. E. Bridges, "Wideband Ultralow Reverberation Antenna for Biological Sensing," *Electron. Lett.*, vol. 33, no. 19 (Sept. 1997): 1594–1595.

36. M. A. Hernandez-Lopez, M. Pantoja, M. Fernandez, S. Garcia, A. Bretones, R. Martin, and R. Gomez, "Design of an Ultra-broadband V Antenna for Microwave Detection of Breast Tumors," *Microw. Opt. Tech. Lett.*, vol. 34, no. 3 (Aug. 2002): 164–166.

37. E. C. Fear and M. A. Stuchly, "Microwave Breast Tumor Detection: Antenna Design and Characterization," *IEEE Antennas Propag. Symp. Dig.*, vol. 2 (2000): 1076–1079.

38. X. Li, S. C. Hagness, M. K. Choi, and D. W. W. Choi, "Numerical and Experimental Investigation of an Ultrawideband Ridged Pyramidal Horn Antenna with Curved Launching Plane for Pulse Radiation," *IEEE Antennas Wireless Propag. Lett.*, vol. 2 (2003): 259–262.

39. X. Yun, E. C. Fear, and R. H. Johnston, "Radar-based Microwave Imaging for Breast Cancer Detection: Tumor Sensing with Cross-Polarized Reflections," *IEEE Antennas Propag. Society Symp. Dig.*, vol. 3 (2004): 2432–2435.

40. C. J. Shannon, E. C. Fear, and M. Okoniewski, "Dielectric-Filled Slotline Bowtie Antenna for Breast Cancer Detection," *Electronics Letters*, vol. 41, no. 7 (March 2001).

41. J. M. Sill and E. C. Fear, "Tissue Sensing Adaptive Radar for Breast Cancer Detection: A Study of Immersion Liquid," *Electron. Lett.*, vol. 41, no. 3 (Feb. 2005): 113–115.

42. J. M. Sill and E. C. Fear, "Tissue Sensing Adaptive Radar for Breast Cancer Detection: Preliminary Experimental Results," IEEE MTT-S Int. Microwave Symp. Dig., Long Beach, CA, June 2005.

43. J. M. Sill and E. C. Fear, "Tissue Sensing Adaptive Radar for Breast Cancer Detection—Experimental Investigation of Simple Tumor Models," *IEEE Trans. Microwave Theory Tech.*, vol. 53, no. 11 (Nov. 2005): 3312–3319.

44. D. M. Sullivan, "Three-dimensional Computer Simulation in Deep Regional Hyperthermia Using the FDTD Method," *IEEE Trans. Microwave Theory and Tech.*, vol. 38, no. 2 (Feb. 1990): 201–211.
45. B. M. Green and M. A. Jensen, "Diversity Performance of Dual-Antenna Handsets Near Operator Tissue," *IEEE. Trans. Antennas and Propagation*, vol. 48, no. 7 (July 2000): 1017–1024.
46. O. Gandhi, G. Lazzi, and C. Furse, "Electromagnetic Absorption in the Human Head and Neck for Mobile Telephones at 835 and 1900 MHz," *IEEE Trans. on Microwave Theory and Techn.*, vol. 44 (1996): 1884–1897.
47. P. Soontornpipit, C. M. Furse, and Y. C. Chung, "Design of Implantable Microstrip Antenna for Communication with Medical Implants," Special Issue of *IEEE Trans. on Microwave Theory and Techn.* on Medical Applications and Biological Effects of RF/Microwaves (Sept. 2004).
48. C. E. Reuter, A. Taflove, V. Sathiaseelan, M. Piket-May, and B. B. Mittral, "Unexpected Physical Phenomena Indicated by FDTD Modeling of the Sigma-60 Deep Hyperthermia Applicator," *IEEE Trans. Microwave Theory and Tech.*, vol. 46, no. 4 (April 1998): 313–319.
49. D. Sullivan, D. Buechler, and F. A. Gibbs, "Comparison of Measured and Simulated Data in an Annular Phased Array Using an Inhomogeneous Phantom," *IEEE Trans. Microwave Theory and Tech.*, vol. 40, no. 3 (March 1992): 600–604.
50. C. M. Furse, J.-Y. Chen, and O. P. Gandhi, "Use of the Frequency-Dependent Finite-Difference Time-Domain Method for Induced Current and SAR Calculations for a Heterogeneous Model of the Human Body," *IEEE Transactions on Electromagnetic Compatibility* (May 1994): 128–133.
51. C. Furse and O. P. Gandhi, "Calculation of Electric Fields and Currents Induced in a Millimeter-Resolution Human Model at 60 Hz Using the FDTD Method," *Bioelectromagnetics*, vol. 19, no. 5 (1998): 293–299.
52. C. M. Furse and O. P. Gandhi, "A Memory Efficient Method of Computing Specific Absorption Rate in CW FDTD Simulations," *IEEE Transactions on Biomedical Engineering*, vol. 43, no. 5 (May 1996): 558–560.
53. C. H. Durney, C. C. Johnson, P. W. Barber, H. Massoudi, M. F. Iskander, J. L. Lords, D. K. Ryser, S. J. Allen, and J. C. Mitchell, *Radiofrequency Radiation Dosimetry Handbook*, 2nd Ed. (Brooks AFB, TX: USAF School of Medicine, 1978).
54. O. P. Gandhi, Y. G. Gu, J. Y. Chen, and H. I. Bassen, "Specific Absorption Rates and Induced Current Distributions in an Anatomically Based Human Model for Plane-Wave Exposures," *Health Physics*, vol. 63, no. 3 (1992): 281–290.
55. O. P. Gandhi and C. M. Furse, "Millimeter-Resolution MRI-based Models of the Human Body for Electromagnetic Dosimetry from ELF to Microwave Frequencies," *Voxel Phantom Development: Proc. of an International Workshop*, Peter J. Dimbylow (ed.), National Radiological Protection Board, Chilton, UK, July 6–7, 1995.
56. P. J. Dimbylow, "The Development of Realistic Voxel Phantoms for Electromagnetic Field Dosimetry," *Voxel Phantom Development: Proc. of an International Workshop*, Peter J. Dimbylow (ed.), National Radiological Protection Board, Chilton, UK, July 6–7, 1995.
57. P. Olley and P. S. Excell, "Classification of a High Resolution Voxel Image of a Human Head," *Voxel Phantom Development: Proc. of an International Workshop* held at the National Radiological Protection Board, Chilton, UK, July 6–7, 1995, Peter J. Dimbylow (ed.).
58. M. A. Stuchly, K. Caputa, A. van Wensen, and A. El-Sayed, "Models of Human and Animal Bodies in Electromagnetics," *Voxel Phantom Development: Proc. of an International Workshop*, Peter J. Dimbylow (ed.), National Radiological Protection Board, Chilton, UK, July 6–7, 1995.
59. National Library of Medicine, Visible Man Project, MRI scans, CT scans, and photographs available on CD-ROM through Research Systems, Inc., 2995 Wilderness Place, Boulder, CO 80301.
60. C. Gabriel, S. Gabriel, and E. Corthout, "The Dielectric Properties of Biological Tissues: I. Literature survey," *Phys. Med. Biol.*, vol. 41 (1996): 2231–2249.
61. S. Gabriel, R. W. Lau, and C. Gabriel, "The Dielectric Properties of Biological Tissues: II. Measurements on the Frequency Range 10 Hz to 20 GHz," *Phys. Med. Biol.*, vol. 41 (1996): 2251–2269.

62. S. Gabriel, R. W. Lau, and C. Gabriel. "The Dielectric Properties of Biological Tissues: III. Parametric Models for the Dielectric Spectrum of Tissues," *Phys. Med. Biol.*, vol. 41 (1996): 2271–2293.

63. K. R. Foster and H. P. Schwan, "Dielectric Properties of Tissues and Biological Materials: A Critical Review," *Crit. Rev. Biomed. Eng.*, vol. 17 (1989): 25–104.

64. S. S. Chaudhary, R. K. Mishra, A. Swarup, and J. M. Thomas, "Dielectric Properties of Normal and Malignant Human Breast Tissues at Radiowave and Microwave Frequencies," *Indian J. Biochem. Biophys.*, vol. 21 (1984): 76–79.

65. A. J. Surowiec, S. S. Stuchly, J. R. Barr, and A. Swarup, "Dielectric Properties of Breast Carcinoma and the Surrounding Tissues," *IEEE Trans. Biomed. Eng.*, vol. 35 (April 1988): 257–263.

66. W. T. Joines, Y. Z. Dhenxing, and R. L. Jirtle. "The Measured Electrical Properties of Normal and Malignant Human Tissues from 50 to 900 MHz," *Med. Phys.*, vol. 21 (1994): 547–550.

67. A. M. Campbell and D. V. Land, "Dielectric Properties of Female Human Breast Tissue Measured in Vitro at 3.2 GHz," *Phys. Med. Biol.*, vol. 37 (1992): 193–210.

68. C. Gabriel, "Compilation of the Dielectric Properties of Body Tissues at RF and Microwave Frequencies," Final Report AL/OE-TR-1996-0037 submitted to Occupational and Environmental Health Directorate, RFR Division, 2503 Gillingham Dr., Brooks AFB, TX, June 1996.

69. M. A. Stuchly and S. S. Stuchly, "Dielectric Properties of Biological Substances – Tabulated," *J. Microwave Power*, vol. 15, no. 1 (1980): 19–26.

70. S. Rush, J. A. Abildskov, and R. McFee, "Resistivity of Body Tissues at Low Frequencies," *Circ. Research*, vol. XII (1963): 40–50.

71. L. A. Geddes and L. E. Baker, "The Specific Resistance of Biological Material—A Compendium of Data for the Biomedical Engineer and Physiologist," *Med. & Biol. Eng.*, vol. 5 (1967): 271–293.

72. University of Utah Dielectric Database OnLine, http://www.ece.utah.edu/dielectric/.

73. D. Colton and P. Monk, "A New Approach to Detecting Leukemia: Using Computational Electromagnetics," *IEEE Trans. Comput. Sci. Eng.*, vol. 2 (Winter 1995): 46–52.

74. S. Y. Semenov, A. E. Bulyshev, A. E. Souvorov, R. H. Svenson, Y. E. Sizov, V. Y. Borisov, V. G. Posukh, I. M. Kozlov, A. G. Nazarov, and G. P. Tatsis, "Microwave Tomography: Theoretical and Experimental Investigation of the Iteration Reconstruction Algorithm," *IEEE Trans. Micr. Theory Tech.*, vol. 46 (Feb. 1998): 133–141.

75. S. Y. Semenov, R. H. Svenson, A. E. Bulyshev, A. E. Souvorov, A. G. Nazarov, Y. E. Sizov, V. G. Posukh, and A. Pavlovsky, "Three-Dimensional Microwave Tomography: Initial Experimental Imaging of Animals," *IEEE Trans. Biomed. Eng.*, vol. 49 (Jan. 2002): 55–63.

76. K. L. Carr, "Microwave Radiometry: Its Importance to the Detection of Cancer," *IEEE Trans. Microwave Theory Tech.*, vol. 37, no. 12 (Dec. 1989): 1862–1869.

77. K. L. Carr, "Radiometric Sensing," *IEEE Potentials* (April/May 1997): 21–25.

78. L. Dubois, J.-P. Sozanski, V. Tessier, J.-C. Camart, J.-J. Fabre, J. Pribetich, and M. Chiv, "Temperature Control and Thermal Dosimetry by Microwave Radiometry in Hyperthermia," *IEEE Trans. Microwave Theory Tech.*, vol. 44, no. 10 (Oct. 1996): 1755–1761.

79. S. M. Fraser, D. V. Land, and R. D. Sturrock, "Microwave Thermography—an Index of Inflammatory Disease," *Br. J. Rheumatology*, vol. 26 (1987): 37–39.

80. B. Bocquet, J. C. Van de Velde, A. Mamouni, and Y. Leroy, "Microwave Radiometric Imaging at 3 GHz for the Exploration of Breast Tumours," *IEEE Trans. Microwave Theory Tech.*, vol. 38 (1990): 791–793.

81. J. Robert, J. Edrich, P. Thouvenot, M. Gautherie, and J. M. Escanye, "Millimeter Wave Thermography: Preliminary Clinical Finding on Head and Neck Diseases," *J. Microwave Power*, vol. 14 (1979).

82. K. L. Carr, A. M. El Mahdi, and J. Schaeffer, "Dual Mode Microwave System to Enhance Early Detection of Cancer," *IEEE Trans. Microwave Theory Tech.*, vol. 29 (1980): 256–260.

83. E. A. Cheever, J. B. Leonard, and K. R. Foster, "Depth of Penetration of Fields from Rectangular Apertures into Lossy Media," *IEEE Trans. Microwave Theory Tech.*, vol. 35 (1987): 865–867.

84. J. Audet, J. C. Bolomey, C. Pichot, D. D. n'Guyen, M. Robillard, M. Chive, and Y. Leroy, "Electrical Characteristics of Waveguide Applicators for Medical Applications," *J. Microwave Power*, vol. 15 (1980): 177–186.

85. A. W. Guy, "Electromagnetic Fields and Relative Heating Patterns Due to a Rectangular Aperture Source in Direct Contact with Bilayered Biological Tissue," *IEEE Trans. Microwave Theory Tech.*, vol. 29 (1971): 214–223.

86. D. V. Land, "Medical Microwave Radiometry and Its Clinical Applications," *IEE Colloquium Application of Microwaves in Medicine* (28 Feb. 1995): 2/1–2/5.

87. B. Enander and G. Larson, "Microwave Radiometry Measurements of the Temperature Inside a Body," *Electronic Letters*, vol. 10 (1974): 317.

88. J. Edrich and P. C. Hardee, "Thermography at Millimeter Wavelengths," *Proc. IEEE*, vol. 62 (1974): 1391–1392.

89. E. A. Cheever and K. R. Foster, "Microwave Radiometry in Living Tissue: What Does It Measure?" *IEEE Trans. Biomedical Engineering*, vol. 39, no. 6 (June 1992): 563–568.

90. B. Bocquet, J. C. van de Velde, A. Mamouni, Y. Leroy, G. Giauz, J. Delannoy, and D. Delvalee, "Microwave Radiometric Imaging at 3 GHz for the Exploration of Breast Tumors," *IEEE Trans. Microwave Theory Tech.*, vol. 38, no. 6 (June 1990): 791–793.

91. L. Enel, Y. Leroy, J. C. Van de Velde, and A. Mamouni, "Improved Recognition of Thermal Structures by Microwave Radiometry," *Electron. Lett.*, vol. 20 (1984): 293–294.

92. Y. Leroy, A. Mamouni, J. C. Van de Velde, B. Bocquet, and B. Dujardin, "Microwave Radiometry for Noninvasive Thermometry," *Automedica* (special issue on noninvasive thermometry), vol. 8 (1987): 181–201.

93. C. E. Hayes, W. A. Edelstein, J. F. Schenck, et al, "An Efficient, Highly Homogeneous Radiofrequency Coil for Whole-body NMR Imaging at 1.5 T," *J. Magn. Reson. Imaging*, vol. 63 (1985): 622–628.

94. M. C. Leifer, "Theory of the Quadrature Elliptic Birdcage Coil," *Magn. Reson. Med.*, vol. 38 (1997): 726–732.

95. S. Li, C. M. Collins, B. J. Dardzinski, et al, "A Method to Create an Optimum Current Distribution and Homogeneous B1 Field for Elliptical Birdcage Coils," *Magn. Reson. Med.*, vol. 37 (1997): 600–608.

96. J. R. Fitzsimmons, J. C. Scott, D. M. Peterson, et al, "Integrated RF Coil with Stabilization for FMRI Human Cortex," *Magn. Reson. Med.*, vol. 38 (1997): 15–18.

97. L. E. Hendrix, J. A. Strandt, D. L. Daniels, et al, "Three-Dimensional Time-of-Flight MR Angiography with a Surface Coil: Evaluation in 12 Subjects," *American Journal Radiology*, vol. 159 (1992): 103–106.

98. P. B. Roemer, W. A. Edelstein, C. E. Hayes, S. P. Souza, and O. M. Mueller, "The NMR Phased Array," *Magn. Reson. Med.*, vol. 16, no. 2 (1996): 192–225.

99. C. E. Hayes, N. Hattes, and P. B. Roemer, "Volume Imaging with MR Phased Arrays," *Magn. Reson. Med.*, vol. 18, no. 2 (1991): 309–319.

100. C. E. Hayes and P. B. Roemer, "Noise Correlations in Data Simultaneously Acquired from Multiple Surface Coil Arrays," *Magn. Reson. Med.*, vol. 16, no. 2 (1991): 181–191.

101. S. M. Wright, R. L. Magin, and J. R. Kelton, "Arrays of Mutually Coupled Receiver Coils: Theory and Application," *Magn. Reson. Med.*, vol. 17, no. 1 (1991): 252–268.

102. S. M. Wright and L. L. Wald, "Theory and Application of Array Coils in MR Spectroscopy," *NMR Biomed*, vol. 10, no. 8 (1997): 394–410.

103. G. R. Duensing, H. R. Brooker, and J. R. Fitzsimmons, "Maximizing Signal-to-Noise Ratio in the Presence of Coil Coupling," *J. Magn. Reson. B.*, vol. 111, no. 3 (1996): 230–235.

104. D. K. Sodickson and W. J. Manning, "Simultaneous Acquisition of Spatial Harmonics (SMASH): Ultra-fast Imaging with Radiofrequency Coil Arrays," *Magn. Reson. Med.*, vol. 38 (1997): 591–603.

105. K. P. Pruessmann, M. Weiger, M. B. Scheidegger, and P. Boesiger, "SENSE: Sensitivity Encoding for Fast MRI," *Magn. Reson. Med.*, vol. 42 (1999): 952–962.

106. Y. Zhu, "Parallel Excitation with an Array of Transmit Coils," *Magn. Reson. Med.*, vol. 51, no. 4 (2004): 775–784.

107. K. Y. Kojima, J. Szumowski, R. C. Sheley, et al, "Lower Extremities: MR Angiography with a Unilateral Telescopic Phased-Array Coil," *Radiology*, vol. 196 (1995): 871–875.

108. J. W. Monroe, P. Schmalbrock, and D. G. Spigos, "Phased Array Coils for Upper Extremity MRA," *Magn. Reson. Med.*, vol. 33 (1995): 224–229.

109. C. E. Hayes, C. M. Mathis, and C. Yuan, "Surface Coil Phased Arrays for High-Resolution Imaging of the Carotid Arteries," *J. Magn. Reson. Imaging*, vol. 1 (1996): 109–112.

110. C. Yuan, J. W. Murakami, C. E. Hayes, et al, "Phased-Array Magnetic Resonance Imaging of the Carotid Artery Bifurcation: Preliminary Results in Healthy Volunteers and a Patient with Atherosclerotic disease," *J. Magn. Reson. Imaging*, vol. 5 (1995): 561–565.

111. S. H. Faro, S. Vinitski, H. V. Ortega, et al, "Carotid Magnetic Resonance Angiography: Improved Image Quality with Dual 3-inch Surface Coils," *Neuroradiology*, vol. 38 (1996): 403–408.

112. H. A. Stark and E. M. Haacke, "Helmet and Cylindrical Shaped CP Array Coils for Brain Imaging: a Comparison of Signal-to-Noise Characteristics," *Proceedings of the International Society for Magnetic Resonance in Medicine* (1996): 1412.

113. J. R. Porter, S. M. Wright, and A. Reykowski, "A 16-Element Phased-Array Head Coil," *Magn. Reson. Med.*, vol. 40 (1998): 272–279.

114. T. Wu and R. King, "The Cylindrical Antenna with Nonreflecting Resistive Loading," *IEEE Trans. Antennas Propag.*, vol. AP-13, no. 3 (May 1965): 369–373.

115. T. Wu and R. King, "Corrections to 'The Cylindrical Antenna with Nonreflecting Resistive Loading'," *IEEE Trans. Antennas Propag.*, vol. AP-13, no. 11 (Nov. 1965): 998.

116. E. C. Fear, J. Sill, and M. A. Stuchly, "Experimental Feasibility Study of Confocal Microwave Imaging for Breast Tumor Detection," *IEEE Trans. Microwave Theory Tech.*, vol. 51, no. 3 (March 2003): 887–892.

117. Special Issue of *IEEE Trans. Microwave Theory Tech.*, MTT-34, 1986.

118. C. H. Durney and M. F. Iskander, *Antenna Handbook*, Y. T. Lo and S. W. Lee (eds.) (New York: Springer, 1993).

119. P. K. Sneed and T. L. Phillips, "Combining Hyperthermia and Radiation: How Beneficial?," *Oncology*, vol. 5 (1991): 99–108.

120. C. C. Vernon, J. W. Hand, S. B. Field, et al, "Radiotherapy with or Without Hyperthermia in the Treatment of Superficial Localized Breast Cancer: Results from Five Randomized Controlled Trials," *Int. J. Radiat. Oncol. Biol. Phys.*, vol. 35 (1996): 731–44.

121. F. Monteccia, "Microstrip Antenna Design for Hyperthermia Treatment of Superficial Tumors," *IEEE Trans. BME*, vol. 39, no. 6 (June 1992): 580–588.

122. J. Vba, C. Franconi, F. Montecchia, and I. Vannucci, "Evanescent-Mode Applicators (EMA) for Superficial and Subcutaneous Hyperthermia," *IEEE Trans. Biomed. Eng.*, vol. 40, no. 5 (May 1993): 397–407.

123. M. V. Prior, M. L. D. Lumori, J. W. Hand, G. Lamaitre, C. J. Schneider, and J. D. P. van Dijk, "The Use of a Current Sheet Applicator Array for Superficial Hyperthermia: Incoherent Versus Coherent Operation," *IEEE Trans. Biomed. Eng.*, vol. 43, no. 7 (July 1995): 694–698.

124. J. Bach Andersen, A. Baun, K. Harmark, L. Heinz, P. Raskmark, and J. Overgaard, "A Hyperthermia System Using a New Type of Inductive Applicator," *IEEE Trans. Biomedical Engineering*, vol. 31(1), (1984): 21–27.

125. P. R. Stauffer, M. Leoncini, V. Manfrini, et al, "Dual Concentric Conductor Radiator for Microwave Hyperthermia with Improved Field Uniformity to Periphery of Aperture," *IEICE Trans. on Communicat.*, vol. E78-B (1995): 826–35.

126. P. F. Maccarini, H. Rolfsnes, D. Neuman, and P. Stauffer, "Optimization of a Dual Concentric Conductor Antenna for Superficial Hyperthermia Applications," Proceedings of the 26th Annual International Conference of the IEEE EMBS, San Francisco, CA, Sept. 1–5, 2004.

127. H. Tehrani and K. Chang, "Multifrequency Operation of Microstrip Fed Slot Ring Antennas on Thin Low Dielectric Permittivity Substrates," *IEEE Trans. on Antennas and Propagation.*, vol. 50, no. 9 (Sept. 2002): 1299–1308.

128. S. Jacobsen, P. R. Stauffer, and D. G. Neuman, "Dual-Mode Antenna Design for Microwave Heating and Noninvasive Thermometry of Superficial Tissue Disease," *IEEE Trans. Biomed. Eng.*, vol. 47 (2000): 1500–9.

129. P. F. Turner, "Interstitial Equal-Phased Arrays for EM Hyperthermia," *IEEE Trans. Micr. Theory and Tech.*, vol. 34, no. 5 (May 1986): 572–578.

130. R. D. Nevels, G. D. Arndt, G. W. Raffoul, J. R. Carl, and A. Pacifico, "Microwave Catheter Design," *IEEE Trans. Biomed. Eng.*, vol. 45 (July 1998): 885–890.

131. C. Manry, S. L. Broschat, C.-K. Chou, and J. A. McDougall, "An Eccentrically Coated Asymmetric Antenna Applicator for Intracavity Hyperthermia Treatment of Cancer," *IEEE Trans. Biomed. Eng.*, vol. 39, no. 9 (Sept. 1992): 935–942.

132. P. F. Turner, "Hyperthermia and Inhomogeneous Tissue Effects Using an Annular Phased Array," *IEEE Trans. Microwave Theory and Tech.*, vol. 32, no. 8 (Aug. 1984): 874–875.

133. P. Stauffer, J. Schlorff, R. Taschereau, T. Juang, D. Neuman, P. Maccarini, J. Pouliot, and J. Hsu, "Combination Applicator for Simultaneous Heat and Radiation," Proceedings of the 26th Annual International Conference of the IEEE EMBS, San Francisco, CA, Sept. 1–5, 2004.

134. Y. Kotsuka, E. Hankui, and Y. Shigematsu, "Development of Ferrite Core Applicator System for Deep-Induction Hyperthermia," *IEEE Trans. Micr. Theory and Tech.*, vol. 44, no. 10 (Oct. 1996): 1803–1810.

135. P. F. Turner, "Sigma 60–24 Prototype Test Results," BSD Medical Corporation, Internal Rep., Salt Lake City, UT, 1992.

136. J. Nadobny, H. Fähling, M. Hagmann, P. Turner, W. Wlodarczyk, J. Gellermann, P. Deuflhard, and P. Wust, "Experimental and Numerical Investigations of Feed-Point Parameters in a 3-D Hyperthermia Applicator Using Different Models of Feed Networks," *IEEE Trans. Biomed. Eng.*, vol. 49, no. 11 (Nov. 2002): 1348–1359.

137. J. Nadobny, W. Wlodarczyk, L. Westhoff, J. Gellermann, R. Felix, and P. Wust, "A Clinical Water-Coated Antenna Applicator for MR-Controlled Deep-Body Hyperthermia: A Comparison of Calculated and Measured 3-D Temperature Data Sets," *IEEE Trans. Biomed. Eng.*, vol. 52, no. 3 (March 2005): 505–519.

138. K. S. Nikita and N. K. Uzunoglu, "Coupling Phenomena in Concentric Multi-Applicator Phased Array Hyperthermia Systems," *IEEE Trans. Microwave Theory and Tech.*, vol. 44, no. 1 (Jan. 1996): 65–74.

139. F. Bardati, A. Borrani, A. Gerardino, and G. A. Lovisolo, "SAR Optimization in a Phased Array Radiofrequency Hyperthermia System," *IEEE Trans. Biomed. Eng.*, vol. 42, no. 12 (Dec. 1995): 1201–1207.

140. R. G. Olsen, M. B. Ballinger, T. D. David, and W. G. Lotz, "Rewarming of the Hypothermic Rhesus Monkey with Electromagnetic Radiation," *Bioelectromagnetics*, vol. 8 (1987): 183–193.

141. I. D. McRury and D. E. Haines, "Ablation for the Treatment of Arrhythmias," *Proceedings of the IEEE*, vol. 84, no. 3: 404–416.

142. A. Labonte, A. Blais, S. Legault, H. O. Ai, and L. Roy, "Monopole Antennas for Microwave Catheter Ablation," *IEEE Trans. on Microwave Theory and Techn.*, vol. 44, no. 10: 1832–1840.

143. A. Rosen et al, "Percutaneous Transluminal Microwave Balloon Angioplasty," *IEEE Trans. Microwave Theory Tech.*, vol. 38 (1990): 90–93.

144. A. J. Johansson, "Simulation and Verification of Pacemaker Antennas," Proceedings of the 25th Annual Int. Conf. of the IEEE EMBS, Cancun, Mexico, Sept. 17–21, 2003.

145. K. Guillory and R. A. Normann, "A 100-Channel System for Real Time Detection and Storage of Extracellular Spike Waveforms," *J. Neurosci. Methods*, vol. 91 (1999): 21–29.

146. T. Buchegger et al, "An Ultra-Low Power Transcutaneous Impulse Radio Link for Cochlea Implants," *Joint Ultra Wideband Systems and Technologies (UWBST) and International Workshop on UWBS 2004*, IEEE cat. no. 04EX812 (2004): 356–360.

147. K. Gosalia, G. Lazzi, and M. Humayun, "Investigation of Microwave Data Telemetry Link for a Retinal Prosthesis," *IEEE Trans. Microwave Theory and Tech.*, vol. 52, no. 8 (Aug. 2004): 1925–1932.

148. C. Furse, "Design an Antenna for Pacemaker Communication," *Microwaves & RF* (March 2000): 73–76.

149. I. J. Bahl, S. S. Stuchly, J. Lagendijk, and M. Stuchly, "Microstrip Loop Applicators for Medical Applications," *IEEE Trans. MTF* (July 1982): 1090–1093.

150. I. J. Bahl, P. Bhartia, and S. S Stuchly, "Design of Microstrip Antennas Covered with a Dielectric Layer," *IEEE Trans. Antennas Propagat.*, vol. AP-30, no. 2 (March 1982): 314–318.

151. R. D. Nevels, D. Arndt, J. Carl, G. Raffoul, and A. Pacifico, "Microwave Antenna Design for Myocardial Tissue Ablation Applications," *IEEE Antennas and Propagat. Soc. Mt. Symp.*, vol. 3 (1995): 1572.

152. C. T. Charles, "Electrical Components for a Fully Implantable Neural Recording System," Master's thesis, Electrical and Computer Engineering, University of Utah, Salt Lake City, Utah, 2003.

153. W. G. Scanlon, N. E. Evans, G. C. Crumley, and Z. M. McCreesh, "Low-Power Radio Telemetry: the Potential for Remote Patient Monitoring," *Journal of Telemedicine and Telecare*, vol. 2, no. 4 (Dec. 1996): 185.

154. W. G Scanlon, N. E. Evans, and Z. M. McCreesh, "RF Performance of a 418 MHz Radio Telemeter Packaged for Human Vaginal Placement," *IEEE Trans. BME*, vol. 44, no. 5 (May 1997): 427–430.

155. W. G Scanlon, N. E. Evans, and J. B. Burns, "FDTD Analysis of Close-Coupled 418 MHz Radiating Devices for Human Biotelemetry," *Physics in Medicine and Biology*, vol. 44, no. 2 (Feb. 1999): 335–345.

156. W. G. Scanlon, J. B. Burns, and N. E. Evans, "Radiowave Propagation from a Tissue-Implanted Source at 418 MHz and 916.5 MHz," *IEEE Trans. Biomedical Engineering*, vol. 47, no. 4 (April 2000): 527–534.

157. G. C. Crumley, N. E. Evans, J. B. Burns, and T. G. Trouton, "On the Design and Assessment of a 2.45 GHz Radio: Telecommand System for Remote Patient Monitoring," *Medical Engineering and Physics*, vol. 20, no. 10 (March 1999): 750–755.

158. C. P. Yue and S. S. Wong, "On-Chip Spiral Inductors with Patterned Ground Shields for Si-based RF IC's," Center for Integrated Systems, Stanford University, 1998.

159. G. S. Brindley and W. S. Lewin, "The Sensations Produced by Electrical Stimulation of the Visual Cortex," *J. Physiol.*, vol. 196 (1968): 479–493.

160. G. E. Loeb, C. J. Samin, J. H. Schulman, and P. R. Troyk, "Injectable Microstimulator for Functional Electrical Stimulation," *Med. Biol. Eng. Comput.*, vol. 29 (1991): NS 13–NS 19.

161. B. Ziaie, M. D. Nardin, A. R. Coghlan, and K. Najafi, "A Single Channel Implantable Microstimulator for Functional Neuromuscular Stimulation," *IEEE Trans. Biomed. Eng.*, vol. 44 (Oct. 1997): 909–920.

162. Weimin Sun et al, Implantable Medical Device Microstrip Telemetry Antenna (Jan. 19, 1999): U.S. Pat. 5,861,019.

163. P. R. Troyk and M. A. K. Schwan, "Closed Loop Class E Transcutaneous Power and Data Link for Microimplants," *IEEE Trans. Biomed. Eng.*, vol. 39 (June 1992): 589–598.

164. G. M. Clark, Y. C. Tong, J. F. Patrick, P. M. Seligman, P. A. Crosby, J. A. Kuzma, and D. K. Money, "A Multi-channel Hearing Prosthesis for Profound-to-Total Hearing Loss," *J. Med. Eng., Technol.*, vol. 8 (Jan. 1984): 3–8.

165. N. de N. Donaldson and T. A. Perkins, "Analysis of Resonant Coupled Coils in Design of Radio Frequency Transcutaneous Links," *Med. Biol. Eng. Comput.*, vol. 21 (Sept. 1983): 612–626.

166. D. C. Galbraith, S. Mani, and R. L. White, "A Wide Band Efficient Inductive Transdermal Power and Data Link with Coupling Insensitive Gain," *IEEE Trans. Biomed. Eng.*, vol. BME-34 (April 1987): 265–275.

167. C. R. Pfaltz (ed.), "The University of Melbourne Nucleus Multi-Electrode Cochlear Implant," *Adv. Oto-Rhino-Laryngol.*, vol. 38 (1987): 63–81.

168. R. S. Mackay, *Bio-Medical Telemetry*, 2nd Ed. (New York: IEEE Press, 1993).

169. A. Johansson, "Wireless Communication with Medical Implants: Antennas and Propagation," PhD dissertation, Lunds Universitet, 2004.

170. M. D. Amundson, J. A. Von Arx, W. J. Linder, P. Rawat, and W. R. Mass, Circumferential Antenna for an Implantable Medical Device (2002): U.S. Pat. 6,456,256

171. L. Griffiths, "Analysis of Wire Antennas for Implantation in the Body," Master's thesis, Utah State University, Logan, UT, 2002.

172. M. Sun, M. Mickle, W. Liang, Q. Liu, and R. J. Sclabassi, "Data Communication Between Brain Implants and Computer," *IEEE Trans. on Neural Systems and Rehabilitation Engineering*, vol. 11, no. 2 (2003): 189–192.

173. P. Soontornpipit, C. M. Furse, and Y. C. Chung, "Design of Implantable Microstrip Antennas for Communication with Medical Implants," *IEEE Trans. MTT*, vol. 52, issue 8 (Aug. 2004): 1944–1951.

174. J. Kim and Y. Rahmat-Samii, "Implanted Antennas Inside a Human Body: Simulations, Designs, and Characterizations," *IEEE Trans. MTT*, vol. 52, issue 8 (Aug. 2004): 1934–1943.

175. K. Gosalia, J. Weiland, M. Humayun, and G. Lazzi, "Thermal Elevation in the Human Eye and Head Due to the Operation of a Retinal Prosthesis," *IEEE Trans. Biomedical Engineering*, vol. 51, no. 8 (Aug. 2004).

176. M. Ghovanloo and G. Lazzi, "Transcutaneous Magnetic Coupling of Power and Data," *Wiley Encyclopedia of Biomedical Engineering*, M. Akay (ed.) (New York: John Wiley & Sons, 2006).

177. C. Furse, G. Lazzi, and O. P. Gandhi, "Dipoles, Monopoles, and Loop Antennas," (invited chapter), *Modern Antennas*, C. Balanis (ed.) (Springer, est. publish date 2007).

178. P. Soontornpipit, C. M. Furse, and Y. C. Chung, "Miniaturized Biocompatible Microstrip Antenna Using Genetic Algorithm," *IEEE Trans. Antennas and Propagat.* (June 2005): 1939–1945.

179. C. A. L. Bassett, "Bioelectromagnetics in the Service of Medicine," *Electromagnetic Fields and Interactions*, Martin Blank, (ed.), American Chemical Society (1995): 262–275.

180. J. C. Weaver, R. Langer, and R. O. Potts, "Tissue Electroporation for Localized Drug Delivery," *Electromagnetic Fields and Interactions*, Martin Blank (ed.), American Chemical Society (1995): 301–316.

181. F. Sterzer, "Microwave Medical Devices," *IEEE Microwave Magazine* (March 2002): 65–70.

182. E. C. Burdette, F. L. Cain, and J. Seals, "In Vivo Probe Measurement Technique for Determining Dielectric Properties at VHF Through Microwave Frequencies," *IEEE Trans. Microwave Theory Tech.*, vol. MTT-28 (April 1980): 414–427.

183. T. K. Bose, A. M. Bottreau, and R. Chahine, "Development of a Dipole Probe for the Study of Dielectric Properties of Biological Substances in Radio Frequency and Microwave Region with Time-Domain Reflectometry," *IEEE Trans. on Instr. and Meas.*, vol. IM-35, no. 1 (March 1986): 56–60.

184. L. Aamodt, M. Manwaring, and K. Manwaring, "In Vivo Brain Tissue Water Measurement," *Proceedings 12th IEEE Symposium on Computer-Based Medical Systems* (June 18–20, 1999): 130–135.

185. H. Bassen and G. Smith, "Electric Field Probes—A Review," *IEEE Transact. on Antennas and Propagat.*, vol. AP-31, no. 5 (Sept. 1983): 710–718.

186. Bassen, "Electric Field Probes for Cell Phone Dosimetry," Proc. 19th International Congress IEEE/EMBS Society, Chicago, Illinois, Oct. 30–Nov. 2, 1997.